U.S. CLIVAR
VARIATIONS
April 2009, Vol. 7, No. 1

Strategic Views

by David M. Legler, Director

The articles in this issue of Variations address a particularly complex and vexing area of ocean-atmospheric coupling in the western boundary ocean current regions. The articles describe some of the difficulties in replicating western boundary currents in coupled climate models, summarize new findings of local and remote effects of the Kuroshio on the ocean and atmosphere, and point out some potential downstream impacts of western boundary currents. These articles highlight just a few of the results of the successful Western Boundary Current Workshop (held in January in Phoenix). More are underway (see article by Cronin in this issue).

Washington continues to undergo a sea of change that started in January. The federal research agencies that support climate research are deciding how to spend Stimulus Package funds (climate research will benefit greatly). They are also considering (in response to a more favorable political environment) how to move forward strategically with a broader agenda to meet the needs of the nation for more information and

Continued on Page Two

IN THIS ISSUE

Local and remote influences of the Kuroshio Extension on the atmosphere

Hiroki Tokinaga[1], Shang-Ping Xie[1,2], Fumiaki Kobashi[3], and Youichi Tanimoto[4]

1 International Pacific Research Center, SOEST, University of Hawaii at Manoa
2 Department of Meteorology, SOEST, University of Hawaii at Manoa
3 Faculty of Marine Technology, Tokyo University of Marine Science and Technology, Tokyo, Japan
4 Graduate School of Environmental Science/Faculty of Environmental Earth Science, Hokkaido University, Sapporo, Japan

Recent satellite studies provide new insights into extratropical ocean-atmosphere interactions. For example, microwave scatteromenter and radiometer observations show that surface wind speed increases over the Kuroshio Extension (KE)'s warm meanders and decreases over detached cold eddies (Nonaka and Xie 2003). Opposite to the conventional view that strong wind cools the ocean surface, this in-phase relationship between SST and wind speed on meso-scales is indicative of an ocean-to-atmospheric influence. Such covariability of SST and surface wind is ubiquitously observed over major SST fronts in the global ocean (see a recent review by Small et al. 2008). Atmospheric soundings with radiosondes and a ceilometer were conducted on several cruises over the Kuroshio Extension to probe the vertical structure of atmospheric adjustments to sharp SST fronts of the KE. This article reviews results from these in-situ (and other satellite) observations over the Northwest Pacific.

Boundary layer response

Weather disturbances frequently pass along the KE front. The presence of sharp SST fronts intensifies temperature and moisture advection across the fronts, which in turn causes sharp transitions in atmospheric stability and vertical structure of the marine atmospheric boundary layer (MABL). Our radiosonde observations capture large MABL variability in associated with cross-frontal advection by weather disturbances. During winter cruises, the near surface atmosphere tended to destabilize (stabilize) on the warmer (colder) flank of the KE front under northerly (southerly) winds. Under unstable stratification, large upward surface heat flux was observed at the sea surface and a well-defined surface mixed layer developed up to 1-2 km high with weak vertical wind shear except in a thin frictional surface layer (Fig. 5 of Tokinaga et al. 2006). This intensified vertical mixing brings large momentum from aloft to accelerate surface wind. The observed vertical adjustments are consistent with the positive correlation between SST and wind speed on meso-scales.

In summer, surface winds are considerably weaker than in winter and the MABL is often capped by a temperature inversion around 1 km high. Summer atmospheric soundings during a Kuroshio Extension System Study (KESS) cruise capture sharp MABL

U.S. CLIMATE VARIABILITY AND PREDICTABILITY (CLIVAR)
1717 Pennsylvania Avenue, NW, Suite 250, Washington, DC 20006• www.usclivar.org

Continued from Page One

knowledge on the impacts of, and response options for, our changing climate. They will be receiving input from the National Academy of Sciences who is soliciting help from a wide cross-section of the researchers and climate knowledge users (see http://americasclimatechoices.org).The America's Climate Choices Panel reports are slated to be released in late 2009.

Moreover, in early April, the Joint Scientific Committee of the World Climate Research Program (WCRP) will be meeting in nearby College Park, Maryland. They hope to identify short-term (to 2013) activities and goals that should be in the forefront of WCRP. They will also consider long-term (post 2013) program scope and directions, ie what should WCRP look like in 2015? The WCRP has been collecting input from its sponsors and supporters as well as from scientists active in its four projects (ie CLIVAR, GEWEX, CLiC, and SPARC). WCRP should be reporting on their delibertions within several months.

It's an exciting time to be involved in climate research. Look for important opportunities and updates on all of these strategic planning efforts in the months ahead.

Variations

Published three times per year
U.S. CLIVAR Office
1717 Pennsylvania Ave., NW
Suite 250, Washington, DC 20006
(202) 419-3471
usco@usclivar.org

Staff: **Dr. David M. Legler**, *Editor*
Cathy Stephens,
Assistant Editor and Staff Writer

This newsletter is supported through contributions to the U.S. CLIVAR Office by NASA, NOAA—Climate Program Office, and NSF.

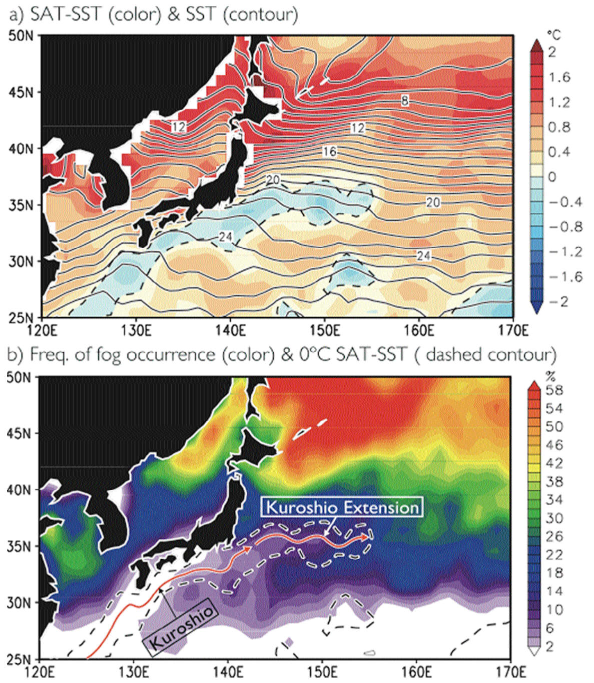

Figure 1. ICOADS (1º x 1º grid) composite for southerly wind cases for the Junes months, 1982-2006 (a) SAT-SST (color in ºC) and SST (contours at 1ºC intervals), and (b) frequency of fog occurrence (color in %). Dashed line is the 0ºC contour of SAT-SST.

transitions across the KE front (Fig. 4 of Tanimoto et al. 2009). Under southerly conditions, the MABL stabilized as warm, humid subtropical air moved across the KE front. A surface inversion and a thick fog layer formed. While the southerlies prevail during summer, northerly winds were occasionally observed when the Baiu rain band was displaced south of the KE. Under northerly conditions, a mixed layer developed capped by stratocumulus clouds with elevated base.

Our analysis of historical ship observations confirms the imprints of ocean fronts on sea fog occurrence. Figure 1 shows the composite map for frequency of fog occurrence and near surface stability (surface air-sea temperature difference, SAT-SST) in June under surface southerly wind conditions. With the southerly warm advection, SAT-SST is positive over most of the domain (Fig. 1a). Over a broad region north of the Oyashio Extension and over the northern Japan Sea, SAT-SST is above 1ºC and the frequency of fog occurrence exceeds 40 % (Fig. 1b). A zonal band of secondary maximum in fog occurrence (> 10 %) extends to the south from 145ºE, 32ºN eastward, corresponding to a positive SAT-SST region on the colder flank of the subtropical SST front. Sandwiched in between are the Kuroshio and its extension where SAT-SST remains weakly negative and the frequency of fog occurrence reaches a meridional minimum (< 10 %). Surface heating by and enhanced vertical mixing over the warm current maintain this band of infrequent fog occurrence.

Deep atmospheric response

Several effects of the KE front may affect the free troposphere above the MABL during winter: (a) intense surface heat flux and (b) surface wind convergence on the warmer flank, and (c) strong baroclinicity (Nakamura et al. 2004). Effects a and b are due to the fact that atmospheric adjustments are of much larger scales than the ocean front (Xie 2004). Together, they help enhance rainfall on the warmer flank of the SST front. This SST frontal effect on precipitation is best seen along the Gulf Stream (Minobe et al. 2008).

Figure 2 shows the enhanced upward surface heat fluxes exceeding 450 W m^{-2} and QuikSCAT wind convergence on the warmer flank of the KE front. Both effects help deepen the clouds, which penetrate above the MABL and frequently reach 500 - 700 hPa in the vertical. Satellite observations of lightning flash rate display a local maximum over the KE region between 143ºE and 155ºE (Fig. 5c of Tokinaga et al. 2009), corroborating the enhanced vertical development of clouds and in good agreement with cyclogenesis along the winter KE front (Figs. 5c and 6c of Hoskins and Hodges 2002).

Signatures of mode water ventilation

Intense heat release to the atmosphere during winter on the warmer flank of the Kuroshio Extension helps form a deep ocean mixed layer and the subtropical mode water (STMW), a thick layer of

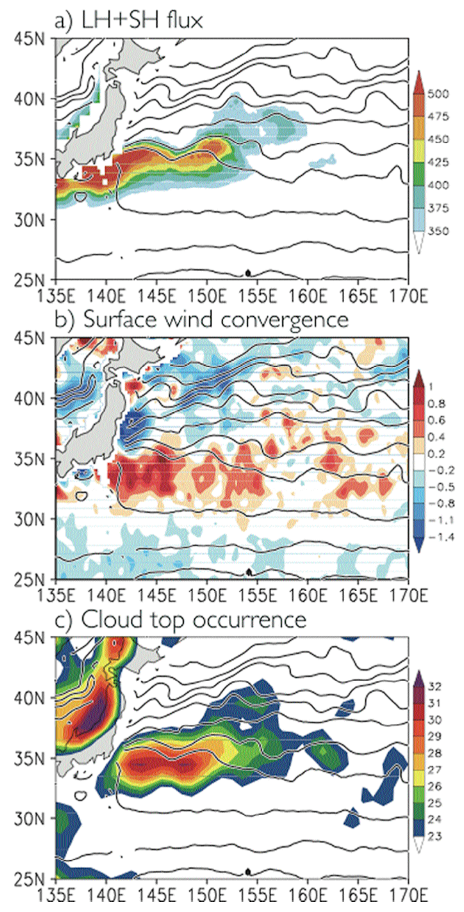

Figure 2. Figure 2. December-February climatology of satellite observations: (a) the sum of upward surface latent and sensible heat fluxes (color in W m^{-2}) from J-OFURO2, (b) QuikSCAT surface wind convergence (color in x 10^{-5} s^{-1}), and (c) cloud top occurrence in the 500 - 700 hPa layer (color in %). Superimposed is AMSR-E SST (contours as 2ºC intervals).

nearly uniform water in the main thermocline. The central mode water (CMW) also forms in the Kuroshio Extension. These mode waters subduct into the permanent thermocline and move southward in the subtropical gyre (Suga et al. 2008). Mode waters of different density eventually stack up in the vertical in the southern subtropical gyre, raising the upper thermocline and forming the Subtropical Countercurrent (STCC) (Kobashi et al. 2006). The STCC is an eastward surface current around 25ºN in the western Pacific, flowing against both the northeast trade winds and the westward Sverdrup flow in the lower thermocline.

The STCC anchors the subtropical front (STF), where deep atmospheric response is observed. QuikSCAT observations reveal that wind stress curls turn slightly cyclonic along the STF in April and May, on the general background of anticyclonic curls in the subtropical gyre (Fig. 2 of Kobashi et al. 2008). The cyclonic wind curls are collocated with a band of high column water vapor content indicative of a deep moist layer. Midlatitude weather disturbances induce subsynoptic-scale low-pressure systems along the STF, fueled by baroclinicity and latent heat release. In these atmospheric lows, convective rain occurs, with deep upward motion moistening the entire troposphere.

Upon subduction, the STMW and CMW are often considered to be insulated from the atmosphere until they circulate back to the KE and outcrop in winter. As the STF illustrates, however, mode waters can leave significant imprints on SST and the atmosphere in the interior ocean before reaching the western boundary. Figure 3 illustrates this atmospheric effect of mode water ventilation in the central subtropical gyre based on a Community Climate System Model version 3 (CCSM3) simulation. The southwest tilted band of the eastward current northwest of Hawaii (around 180º-150ºW, 20º-30ºN) is characteristic of mode-water ventilation in the subtropical gyre (Fig. 3a). This STCC bears a northward component in the midst of southward Sverdrup flow. The northward warm advection by the STCC creates a ridge in SST contours and increases heat flux out of the ocean. (The band of positive heat flux southwest-northeast of Hawaii is due to the cold advection by the northeast trade winds.) Along the SST ridge of STCC, precipitation is locally enhanced, creating a tilted band of reduced Ekman downwelling there (Fig. 3b). The anomalous Ekman upwelling induces a northward Sverdrup current, suggestive of a positive feedback between the STCC and wind stress curl.

Summary

We have briefly reviewed atmospheric effects of the KE in the North Pacific. The ocean fronts enhance thermal advection and cause large cross-frontal variations in atmospheric stability, clouds and other properties of the MABL. We showed evidence based on satellite cloud

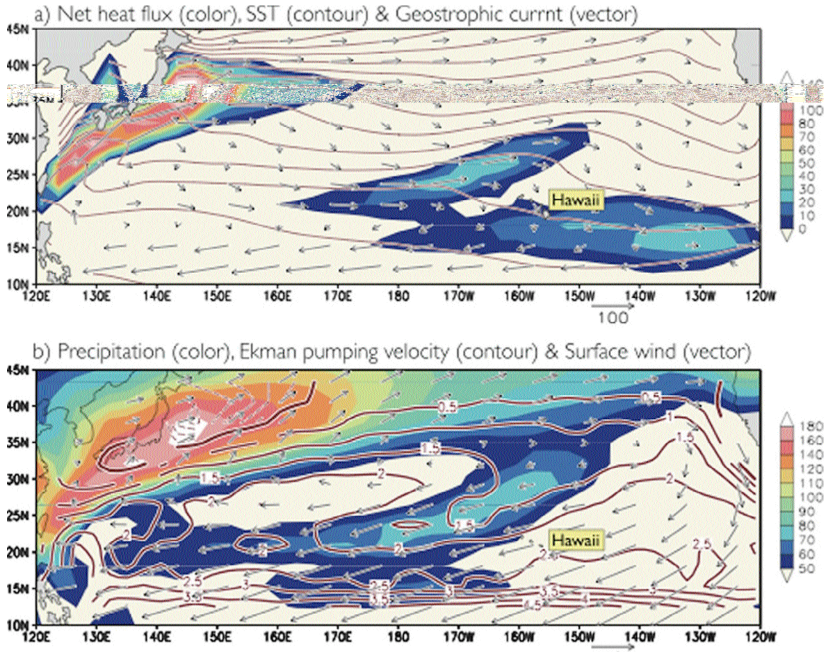

Figure 3. CCSM3-simulated March-May climatology: (a) Net heat flux (color in W m-2), SST (contours at 2ºC intervals) and geostrophic ocean current (vectors; cm s^{-1}), and (b) precipitation (color in mm/month), downward Ekman pumping velocity (contours at 0.5 x 10^{-5} m s^{-1}), and surface wind (vectors; m s^{-1}).

observations for deep atmospheric effects of the KE front, possibly via surface wind convergence, enhanced evaporation, and baroclinic storm growth.

The ventilation of mode waters from the KE is an oceanic teleconnection pathway overlooked in the literature. We showed observational and modeling evidence for its effects on SST, wind and cloud in the interior subtropical gyre. In coarse-resolution (~1°) ocean model hindcasts forced by observed winds, changes in mode water ventilation are the dominant mechanism for subsurface variability in the central subtropical gyre (Xie et al. 2000). In response to increased atmospheric greenhouse forcing, many models project a weakening of North Pacific mode waters, with marked signatures in SST and wind (not shown). Mode water behavior may differ in high-resolution, eddy-resolving models as mesoscale variability affects mode-water formation and mode water, with its potential vorticity minimum, is itself a source of dynamical instability and eddy generation. These issues regarding mode waters and their role in climate need to be further investigated.

Acknowledgments.

This study is supported by NSF, NASA, JSPS, and JAMSTEC.

References:

Hoskins, B. J. and K. I. Hodges, 2002: New perspectives on the Northern Hemisphere winter storm tracks. J. Atmos. Sci., 59, 1041-1061.

Kobashi, F., H. Mitsudera, and S. P. Xie, 2006: Three subtropical fronts in the North Pacific: Observational evidence for mode water-induced subsurface frontogenesis. J. Geophys. Res., 111, C09033, doi: 10.1029/2006JC003479.

Kobashi, F., S.-P. Xie, N. Iwasaka, and T. T. Sakamoto, 2008: Deep atmospheric response to the North Pacific oceanic subtropical front in spring. J. Climate, 21, 5960-5975.

Minobe, S., A. Kuwano-Yoshida, N. Komori, S.-P. Xie, and R. J. Small, 2008: Influence of the Gulf Stream on the troposphere. Nature, 452, 206-U51.

Nakamura, H., T. Sampe, Y. Tanimoto, and A. Shimpo, 2004: Observed associations among storm tracks, jet streams and midlatitude oceanic fronts. Earth's Climate: The Ocean-Atmosphere Interaction, Geophys. Monogr., No. 147, Amer. Geophys. Union, 329–345.

Nonaka, M. and S.-P. Xie, 2003: Covariations of sea surface temperature and wind over the Kuroshio and its extension: Evidence for ocean-to-atmosphere feedback. J. Climate, 16, 1404-1413.

Small, R. J., and Coauthors, 2008: Air-sea interaction over ocean fronts and eddies. Dyn. Atmos. Oceans, 45, 274-319.

Suga, T., Y. Aoki, H. Saito, and K. Hanawa, 2008: Ventilation of the North Pacific subtropical pycnocline and mode water formation. Prog Oceanogr, 77, 285-297.

Tanimoto, Y., and Coauthors, 2009: Observations of marine atmospheric boundary layer transitions across the summer Kuroshio Extension. J. Climate, in press.

Tokinaga, H., and Coauthors, 2006: Atmospheric sounding over the winter Kuroshio Extension: Effect of surface stability on atmospheric boundary layer structure. Geophys. Res. Lett., 33, L04703, doi:10.1029/2005GL025102.

Tokinaga, H., Y. Tanimoto, S.-P. Xie, T. Sampe, H. Tomita, and H. Ichikawa, 2009: Ocean frontal effects on the vertical development of clouds over the western North Pacific: In situ and satellite observations. J. Climate, in press.

Xie, S.-P., 2004: Satellite observations of cool ocean-atmosphere interaction. Bull. Amer. Meteor. Soc., 85, 195-208.

Xie, S.-P., T. Kunitani, A. Kubokawa, M. Nonaka, and S. Hosoda, 2000: Interdecadal thermocline variability in the North Pacific for 1958-97: A GCM simulation. J. Phys. Oceanogr., 30, 2798-2813.

Ocean model representation of western boundary currents and frontal systems: How good are the strongly eddying models?

Matthew W. Hecht
Los Alamos National Laboratory

Western boundary currents are a defining feature of ocean circulation. Any ocean model used in a climate context will produce one. The intensification of the western boundary current occurs because our planet is in rotation, as explained by Stommel (1948).

The western boundary currents and fronts found in the ocean components of climate models, including those appearing in the most recent assessment of the Intergovernmental Panel on Climate Change (IPCC, 2007), suffer from some significant shortcomings. Ocean models used in published climate simulations commonly have grid spacings of around 1°, and produce boundary currents and jets which tend in most cases to be slow, broad and shallow. Underlying these deficiencies is the difficulty of resolving the length scales of oceanic instability: Whereas the size of atmospheric storm systems and the associated atmospheric Rossby radius has been adequately resolved in atmospheric models for years, the much smaller size of the oceanic mesoscale, and of the oceanic Rossby radius of deformation, presents a massive computational challenge to resolve, if one is also interested in the global scale. Eddy feedbacks on the mean circulation may be poorly estimated due to the under-resolved radius of deformation. The models have western boundary currents and many of the observed frontal systems, but they may not be satisfactory representations of what is found in the real ocean.

The slow bias of oceanic jets will

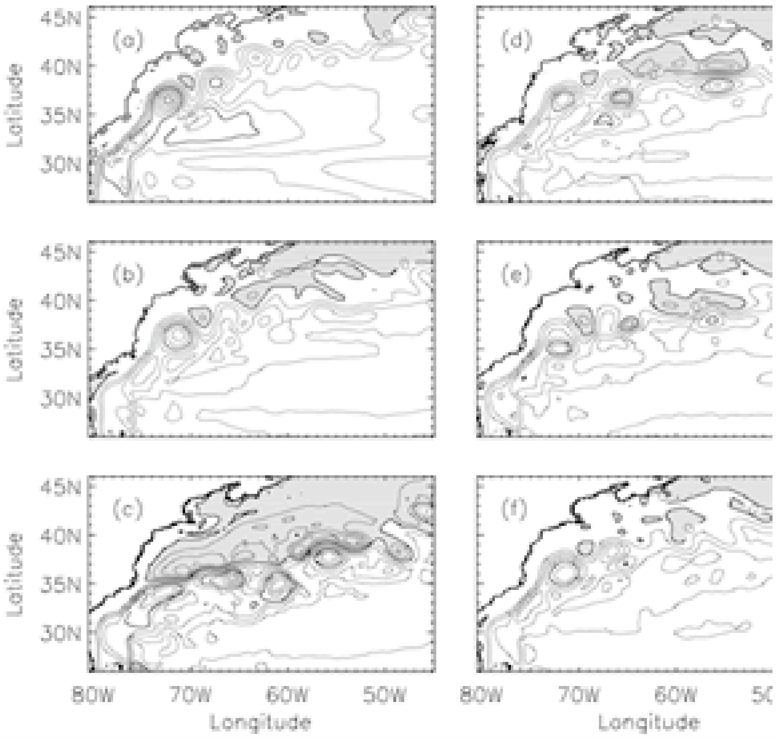

Figure 1. Vertically integrated stream functions, reproduced from Bryan et al. (2007). The left hand column shows the change with increasing resolution, from top (0.4°) to bottom (0.1°), with their usual decrease in lateral dissipation with increasing resolution, as explained therein. Panel (d) shows a poorly separating Gulf Stream at 0.2° resolution, using the lower dissipation that had been used in the higher resolution solution of panel (c). Conversely, panel (e) shows another poorly separating Gulf Stream on the high resolution 0.1° grid, but using the higher dissipation that had been used in the 0.2° simulation of panel (b). The model configuration of panel (f) is the same as that of (e), but with the topographic resolution coarsened to match that of the 0.2° grid.

cause model transit times to be underestimated. The shallowness of currents will tend to reduce the coupling with whatever lies below, be it bathymetry or deeper waters. The breadth of fronts means that a model atmosphere may see an unrealistically relaxed gradient in sea surface temperature. Mean location of fronts, and the variability in frontal location, may also be misrepresented.

A notable exception in present day ocean climate models is the Pacific's equatorial undercurrent, which shows remarkably good structure and realistically high speeds. The greater realism here is partly a result of the attention paid to the modeling of ENSO variability, but is also a consequence of the fact that the Rossby radius becomes large as one approaches the equator. This is the region in which today's climate models can most readily resolve oceanic variability. Indeed, tropical instability waves are found in the better models (Jochum et al., 2008).

Integral transports may be more realistic than the currents themselves, reflecting the robustness of large scale relationships (Sverdrup balance, for example, doesn't depend on mesoscale eddy variability). Poleward heat transports match observations reasonably well, so long as care is taken to respect the extreme difference in magnitude between vertical and lateral (or more precisely dianeutral and isoneutral) diffusivities. In addition to preserving the extremely low values of dianeutral mixing, tracer mixing schemes also parameterize the process of local transfer from potential to kinetic energy which occurs through baroclinic instability.

Eddy variability not only mediates downgradient mixing, but can also be associated with upgradient fluxes, as is the case over much of the Gulf Stream and its Extension (Eden et al. 2007). This aspect of the action of eddy variability has so far eluded parameterization, and is one reason for the poor Gulf Stream System produced by the ocean component of climate models.

At midlatitudes a realistic level of mesoscale variability is obtained at something like 10km or 0.1° grid spacing, a resolution at which the surface expression of mesoscale variability compares well with that derived from satellite altimetry, and a much improved Gulf Stream System may be produced (Bryan et al. 2007). These strongly eddying models have been applied to nearly global (Masumoto et al., 2004) and fully global (Maltrud and McClean, 2005) domains in recent years, and are beginning to be used in ambitious climate modeling efforts. In order to provide a context within which to understand the appropriateness of our most accurate ocean models for the study of air-sea coupling, we briefly review the quality of some of the western boundary currents and frontal systems in strongly eddying models.

Gulf Stream System

The problem of modeling the Gulf Stream is sometimes discussed as one of boundary current separation, where we strive to produce a Stream which separates from the North American coast at the correct location of Cape Hatteras. Smith et al. (2000) produced the first regional North Atlantic simulation with good separation at the Cape, with use of a fine 0.1° grid and fortuitous model configuration (a number of papers referred to therein had indicated that separation might occur with some increase in resolution). Their simulation also produced a northward-flowing North Atlantic Current, rounding the Grand Banks, and an Azores Front.

Lower resolution models, including

all that have been used in published studies of fully-coupled climate to date, tend to produce a Gulf Stream which remains along the coast north of Cape Hatteras, separating as a shallow current which sets up a pronounced anticyclonic meander. These models leave little room for a strong northern recirculation gyre and fail to produce either a northward-flowing North Atlantic Current or an Azores Front. Even with sufficiently high resolution there is still a narrow range of dissipative parameters which allows for development of the full Gulf Stream System, as shown by Bryan et al. (2007). A set of vertically integrated stream functions appears in figure 1, reprinted from their paper, and showing a separating Gulf Stream (c) along with a number of ways to produce a Gulf Stream which fails to separate.

The sensitivity of the Gulf Stream System to model configuration was evident in the first fully global 0.1° simulation, presented by Maltrud and McClean (2005). Late separation of the Gulf Stream is evident in the upper left hand panel of figure 2, reprinted from their paper. The North Atlantic Current also failed to turn north around the Grand Banks (this region is not quite captured in the panel), despite the close similarity between this simulation and the earlier regional simulation of Smith et al. (2000). More recent global modeling efforts have produced an improved Gulf Stream System, as reported in Maltrud et al. (2008), where they credit the improvement to use of a smoother partial bottom cell representation of topography, and to a more regular tripolar horizontal grid discretization.

The problem of Gulf Stream separation is understood as one involving several influences, as described in the review of Dengg et al. (1996). The more recent review of Hecht and Smith (2008) emphasizes the importance of the deep circulation and the need to capture the vertical structure of the Gulf Stream and Deep Western Boundary Current. Deep penetration of the Stream appears to be crucial to formation of a good North Atlantic Current. The climate implications of the absence of a northward flowing NAC (as in climate models, and as also appears to have been the case at the Last Glacial Maximum (Robinson et al., 1995)) was investigated by Weese and Bryan (2006), where they found that a bias in the Azores Low was reduced with correction of the NAC bias.

It is possible, perhaps with some patience, to produce a simulation of the Gulf Stream System with good structure, enabling study of interaction between sea and air in a far more realistic context than was the case only a few years ago.

Kuroshio and its Extension

The Kuroshio is part of a current system that more closely resembles the classic double gyre, with the jet relatively free from topographic influences after its separation from the Japanese coast. As in double gyre studies, the free jet exhibits periods of high and low variability. Jayne et al. (2009) present the first description of the Kuroshio's northern recirculation gyre, and also explain that 2/3 of the transport of the Kuroshio Extension is derived from the recirculation gyres. They report that the average transport of the northern recirculation gyre in the modeling study of Maltrud and McClean (2005) compares well with their analysis of data from the observational array.

In addition to regimes of high and low variability in the Kuroshio Extension, the Kuroshio Current itself also exhibits periods in which a pronounced meander occurs. This meander is clearly evident in the lower right hand panel of figure 2. The meander was far more persistent in the model simulation than in observations, as also appears to have been the case in the nearly-global simulation of Masumoto et al. (2004). This meander in the Kuroshio has been less persistent in the more recent runs of Maltrud et al. (2008). Possible explanations for the improvement include the smoother representation of topography, differences in the parameterization of viscosity, and grid discretization.

Variability in the Kuroshio plays a part in some theories of Pacific Decadal Variability, as for instance in Taguchi et al. (2007). Very recent work points also

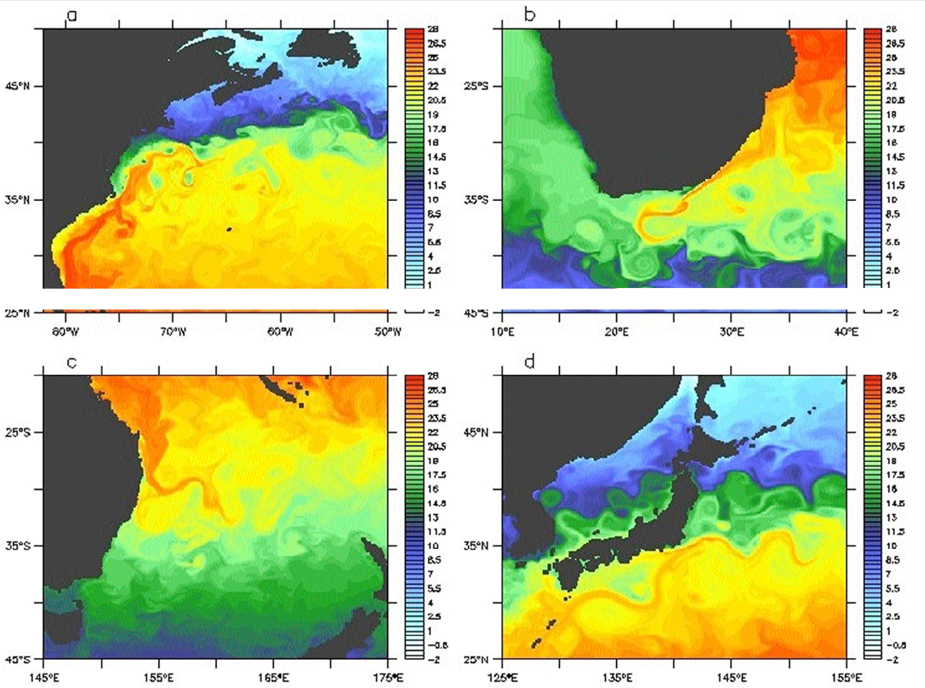

Figure 2. Four western boundary currents are evident in temperature (degrees C) at 15 m depth, from one instant in time (late November) of the 0.1° fully global ocean model simulation of Maltrud and McClean (2005). At upper left is the Gulf Stream, lower left is the East Australia Current, upper right is the Agulhas Retroflection and lower right is the Kuroshio.

to an influence of the Kuroshio on the deep troposphere, as discussed elsewhere in this newsletter, raising the importance of realistic representation of variability in model representation of the current system.

Agulhas

The retroflection of the Agulhas Current is shown in the upper right hand panel of figure 2. Lower resolution ocean climate models have been configured with attention to the large-scale retroflection, but they cannot produce realistically tight gradients in sea surface temperature, nor can they produce the mesoscale turbulence that leads to ring formation. Biastoch et al. (2008) have shown that the resolution of mesoscale turbulence in this region leads to a modulation in Atlantic meridonal overturning circulation which is comparable to that associated with northern deep water formation, a point which has broad consequences for the simulation of Atlantic climate. Lower resolution models fail to capture this southern modulation of the AMOC.

Antarctic Circumpolar Current

The Atlantic Circumpolar region is unique in offering a continuous path around the globe. It stands out as a region where the meridional transport of heat and other properties is performed largely by eddies, and also through its role in connecting the major midlatitude ocean basins, on its northern flank, and the dense waters off Antarctic on its poleward flank.

A great deal of work on the role of eddies has been set in the context of the Atlantic Circumpolar Current, far beyond what can possibly be covered here (a recent and broad presentation is that of Ivchenko et al. (2008)). One question we can take up is the effectiveness of the isopycnal tracer mixing parameterizations (Gent and McWilliams, 1990), the answer to which might address three points:

1. It should allow the model to minimize spurious cross-frontal mixing;
2. meridional eddy transports should be realistic;
3. the feedback of the parameterized effect of mesoscale eddies on the mean flow should also be realistic.

The scheme is very effective at preventing spurious cross-frontal mixing. The value of the mixing parameter may be chosen so that total transport through the Drake Passage falls within observational bounds, which partially addresses points (2) and (3). A study of the oceanic response to changes in wind forcing, performed by Hallberg and Gnanadesikan (2006), indicated that the response is overestimated in a model with parameterized eddies. The parameterization remains extremely valuable, even if it is not a perfectly satisfactory replacement for the action of unresolved mesoscale eddies.

Air-sea interaction over both polar regions is dominated by the extent of sea ice coverage, the simulation of which requires accurate representation of fluxes between ocean and sea ice. The circulation of the Arctic Ocean has yet to be thoroughly studied in a global, strongly eddying context. The first such simulations coupled to active sea ice are now being produced.

Closing remarks

At model resolutions on the order 0.1°, considered to be strongly eddying based on comparison with satellite altimetry, it is possible to produce western boundary current systems and fronts which compare much better with observations, as compared with lower resolution models with parameterized eddies. Interbasin exchanges and influences, including the influence of Agulhas Rings on the Atlantic Meridional Overturning Circulation, as mentioned above, may also be significantly more realistic at high model resolutions. Along with the more direct advantages of well resolved gradients in sea surface temperature and proper location of frontal features, the more subtle issue of the role of mesoscale eddies in the fidelity of the model's response to changes in forcing (illustrated above with results from the Southern Ocean) also offers an advantage to the use of a strongly eddying ocean model.

Acknowledgements

This work was supported by The Climate Change Prediction Program of the Department of Energy's Office of Science. The author also thanks Wilbert Weijer for comments on the text.

References

Biastoch, A., C. W. Boning, and J. Lutjeharms, Agulhas leakage dynamics affects decadal variability in Atlantic overturning circulation, Nature, 456, 489–492, 2008.

Bryan, F. O., M. W. Hecht, and R. D. Smith, Resolution convergence and sensitivity studies with North Atlantic circulation models. Part I: The western boundary current system, Ocean Modelling, 16 (3–4), 141–159, doi:10.1016/j.ocemod.2006.08.005, 2007.

Dengg, J., A. Beckmann, and R. Gerdes, The Gulf Stream separation problem, in The Warmwatersphere of the North Atlantic Ocean, edited by W. Krauss, chap. 9, pp. 253–290, Gebruder Borntraeger, 1996.

Eden, C., R. J. Greatbatch, and J. Willebrand, A diagnosis of thickness fluxes in an eddy-resolving model, J. Phys. Oceanogr., 37 (3), 727–742, doi:10.1175/JPO2987.1, 2007.

Hallberg, R., and A. Gnanadesikan, The role of eddies in determining the structure and response of the wind-driven Southern Hemisphere overturning: Results from the Modeling Eddies in the Southern Ocean (MESO) Project, J. Phys. Oceanogr., 36, 2232–2252, 2006.

Hecht, M. W., and R. D. Smith, Towards a physical understanding of the North Atlantic: A review of model studies in an eddying regime, in Ocean Modeling in an Eddying Regime, edited by M. Hecht and H. Hasumi, no. 177 in Geophysical Monograph Series, pp. 213–239, American Geophysical Union, Washington, D.C., 2008.

Ivchenko, V., S. Danilov, and D. Olbers, Eddies in numerical models of the Southern Ocean, in Ocean Modeling in an Eddying Regime, edited by M. Hecht and H. Hasumi, no. 177 in Geophysical Monograph Series, pp. 177–198, American Geophysical Union, Washington, D.C., 2008.

Jayne, S., et al., The Kuroshio Extension and its recirculation gyres, Deep-Sea Res., submitted, 2009.

Jochum, M., G. Danabasoglu, M. Holland, Y.-O. Kwon, and W. Large, Ocean viscosity and climate, J. Geophys. Res., 113, C06,017, doi:10.1029/2007JC004515, 2008.

Maltrud, M., F. Bryan, M. Hecht, E. Hunke, D. Ivanova, J. McClean, and S.

Peacock, Global ocean modelling in the eddying regime using POP, CLIVAR Exchanges, 44 (1), 5–8, (unpublished manuscript), 2008.

Maltrud, M. E., and J. L. McClean, An eddy resolving 1/10° ocean simulation, Ocean Modelling, 8 (1–2), 31–54, 2005.

Masumoto, Y., et al., A ?fty-year eddy-resolving simulation of the World Ocean: Preliminary outcomes of OFES (OGCM for the Earth Simulator), Journal of the Earth Simulator, 1, 35–56, 2004.

Robinson, S. G., M. A. Maslin, and I. N. McCave, Magnetic-susceptibility variations in Upper Pleistocene deep-sea sediments of the NE Atlantic – Implications for ice rafting and paleocirculation at the Last Glacial Maximum, Paleoceanography, 10 (2), 221–250, 1995.

Smith, R. D., M. E. Maltrud, F. O. Bryan, and M. W. Hecht, Numerical simulation of the North Atlantic Ocean at 1/10°, J. Phys. Oceanogr., 30, 1532–1561, 2000.

Solomon, S., D. Qin, M. Manning, M. Marquis, K. Averyt, M. M. B. Tignor, and H. L. Miller (Eds.), IPCC 2007: Climate Change 2007: The Physical Science Basis. Contribution of Working Group I to the 4th assessment report of the IPCC, p. 996, Cambridge Univ. Press, Cambridge, United Kingdom and New York, NY, USA, 2007.

Stommel, H., The westward intensi?cation of wind-driven ocean currents, Transactions, American Geophysical Union, 29, 202—206, 1948.

Taguchi, B., S.-P. Xie, N. Schneider, M. Nonaka, H. Sasaki, and Y. Sasai, Decadal variability of the Kuroshio Extension: observations and an eddy-resolving model hindcast, J. Clim., 20, 2357–2377, 2007.

Weese, S. R., and F. O. Bryan, Climate impacts of systematic errors in the simulation of the path of the North Atlantic Current, Geophys. Res. Lett., 33 (19), L19,708, doi:10.1029/2006GL027669, 2006.

Atmospheric Sensitivity to SST near the Kuroshio Extension: A Case Study of the Extratropical Transition of Typhoon Tokage

Nicholas Bond, University of Washington/JISAO;
Meghan Cronin, NOAA/Pacific Marine Environmental Laboratory;
Matt Garvert, 3Tier

Tropical cyclones are common in the western North Pacific during late summer and early fall, and many of them include a northward track over the Kuroshio east of Japan. At this stage in their lifecycle, these cyclones typically undergo a transition from tropical to extratropical in nature. It is hypothesized that the tracks and the structural evolutions of these storms during and immediately after their extratropical transitions are sensitive to the underlying sea surface temperature (SST) distribution. While there is a clear local atmospheric response to the marked meridional gradient in SST associated with western boundary currents (e.g., Tokinaga et al. 2006; Minobe et al., 2008), the extent to which it is sensitive to anomalies in SST is controversial (e.g., Kushnir et al. 2002). There is tentative evidence that this sensitivity is mediated by the atmosphere's basic state (e.g., Peng et al. 1997, Bond and Harrison 2000). It is plausible to suppose that extratropical transitions are particularly sensitive to SST, because of the latter's impact on the surface fluxes of sensible and latent heat, which themselves represent the primary energy source for tropical cyclones. One might expect that anomalously warm SSTs would tend to be associated with delayed transitions for storms moving poleward, and that cold SSTs would be associated with hastened transitions, all other factors being equal. The effects of the regional SST on these storms may not have just local manifestations. Modifications in storm properties have potential impacts on the atmospheric circulation over the entire North Pacific basin through the downstream propagation of eddy activity/wave energy (e.g., Chang and Orlanski 1993).

The present contribution on the subject of tropical to extratropical cyclone transition, and in particular the role of the ocean, is based on a series of high-resolution numerical weather prediction (NWP) model simulations of a single storm, Typhoon Tokage in October 2004. This case was selected because of the previous work carried out by Torn and Hakim (2009), who used an ensemble of NWP model simulations to explore the sensitivity of the modeled storm to initial conditions. The control and perturbed SST runs we have carried out also indicate substantial local and remote atmospheric responses to regional SST distributions during the period of Tokage's tropical to extratropical transition.

Methodology

Our analysis is based on simulations carried out with the Weather Research Forecast (WRF3.0) model. All simulations were initialized on 13 October 2004; we have focused on the period of 20-22 October during which Tokage underwent its transition to an extratropical cyclone. The inner nest (15-km grid spacing) for the simulations extends from about 50° to 10° N and from about the dateline to 105° E, i.e., basically the entire western North Pacific. We used such a large domain for the inner nest in order to resolve the mesoscale structure of the cyclone during both its tropical and extratropical phases. Nudging to the operational initializations from NCEP's Global Forecast System (GFS) is applied on an outer domain for the WRF; the latter provides the lateral boundary conditions for the inner domain. The SST distribution used for the control experiment is from the Advanced Microwave Scanning Radiometer (AMSR-E) data set. The

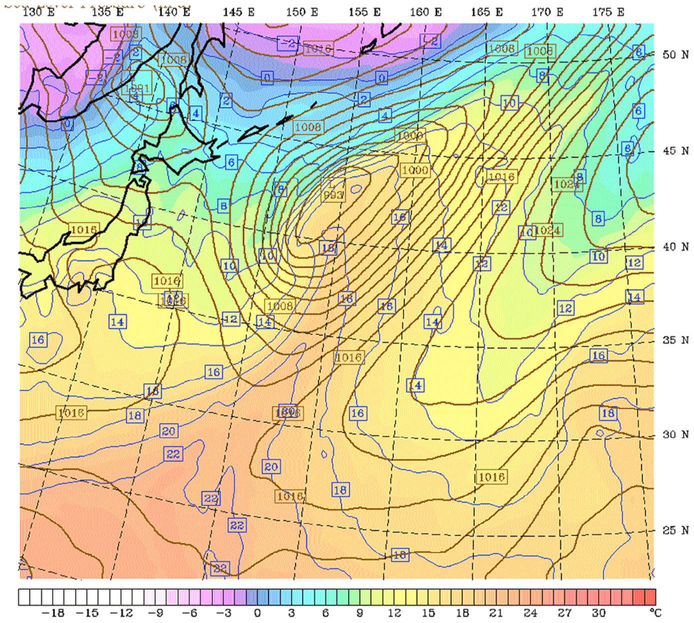

Figure 1 SLP (thick brown lines, contours every 2 hPa) and 925 hPa air temperature (thin blue lines every 2° C with color fills) at 00 UTC 22 October from the control SST simulation.

perturbed SST experiments use the control SST distribution and impose SST anomalies with maximum perturbations of 1.5° C at 35° N, 140° W, tapering off to background values in a Gaussian manner with e-folding scales of 8° in latitude and 16° in longitude (not shown). The shape and magnitude of the SST perturbations resemble the anomalies observed during September through November of 1999-2002, when SSTs were relatively warm in the western North Pacific. The SST perturbations are maintained through the entire duration of the numerical simulations. We focus here on the differences in the modeled atmospheric structure between the control and the positive and negative perturbation SST runs.

Synoptic Review

Based on best track data provided by the Joint Tropical Warning Center (JTWC), the disturbance that became Tokage was first identified as a tropical depression at 7° N, 157° E on 10 October 2004. Tokage gained typhoon status on 13 October and reached its maximum (Category 4) strength on 17 October with a central pressure of 916 hPa and sustained winds of 125 knots. It made landfall in Japan on 20 October on the south side of the island of Shikoku and moved northeast across the central portion of the island of Honshu before moving offshore early on 21 October, at which point the JTWC no longer considered it to be a tropical disturbance. Tokage caused the highest number of casualties (including at least 93 deaths) for a typhoon striking Japan since 1979.

The cyclone that had been Tokage retained considerable strength as it moved northeast and gained increasingly extratropical characteristics. At 00 UTC on 22 October, it was located at 47° N, 161° E and had a central pressure of 990 hPa (NCEP operational analysis; not shown). A key point here is that during the last stages of its tropical phase, and in the early portion of its extratropical phase, the storm's track over the ocean was in the region where SST perturbations were imposed for our NWP model simulations.

SST Perturbation Experiments

The distributions of SLP and 925 hPa air temperature at 00 UTC 22 October for the control simulation are shown in Fig. 1. At this time, the modeled storm has a central SLP of 993 hPa located near 43° N, 154° E. While there is nudging applied on an outer grid, since it is also 9 days into the forecast, it is not surprising that there are errors in central pressure (~3 hPa) and position (~700 km) as compared with the NCEP analysis. We feel that these errors are small enough to consider the control simulation a reasonable representation of the actual situation, especially from a sensitivity perspective.

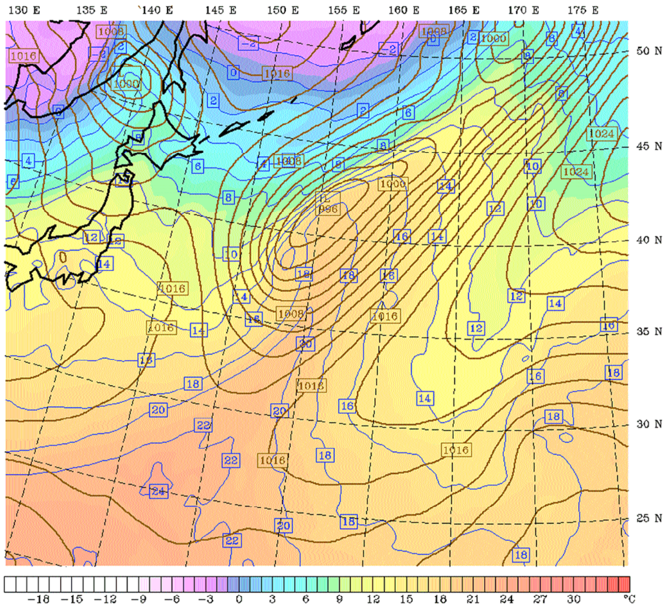

Figure 2 As in Fig. 1, but for the simulation with the warm SST perturbation (see text for details on this perturbation).

The SLP and 925 hPa air temperature distributions at 00 UTC 22 October from the warm SST simulation are shown in Fig. 2. The central pressure is about 996 hPa, or 3 hPa higher than in the control case, and the low center in this perturbed run is located about 70 km to the southeast. The 925 hPa air temperatures are about 1° C greater in the storm's warm sector relative to the control simulation. While the warm front is slightly weaker in the warm SST perturbation relative to the control, the overall low-level storm structure is similar in the two simulations.

The corresponding SLP and 925 hPa air temperature fields for the cold SST simulation (Fig. 3) reveal a substantially different storm. The central pressure of ~983 hPa is 10 hPa lower, and the location of the center at about 44° N 152° E is about 300 km to the

Workshop Spotlight: Western Boundary Currents

Meghan F. Cronin, Michael Alexander, Kathie Kelly, Bo Qiu, and Yolande Serra

The U.S. CLIVAR Western Boundary Current (WBC) Ocean-Atmosphere Interaction Workshop was held on January 15-17, 2009 in Phoenix, AZ. The workshop was sponsored by the U.S. CLIVAR WBC Working Group (WG; http://www.usclivar.org/wbc.php) and the U.S. CLIVAR Program . Approximately 50 scientists from the U.S., Japan, China, France, and Germany attended the workshop, which included 35 oral and 16 poster presentations on topics ranging from observations of air-sea interaction over fronts to global-scale modeling studies.

The overall objective of the workshop was to identify both broad consensus regarding WBC ocean-atmosphere interactions and new provocative ideas and concepts that may affect climate predictability. During the past five years there have been two process studies that have observed WBC dynamics, thermodynamics and interactions with the atmosphere: the Kuroshio Extension System Study (KESS) http://uskess.org, which focused on the Kuroshio Extension in the western North Pacific from June 2004-June 2006; and the CLIvar Mode Water Dynamic Experiment (CLIMODE) http://climode.org which focused on the Gulf Stream in the western North Atlantic from November 2005 – November 2007. At the workshop, KESS and CLIMODE results were presented and there was considerable discussion regarding the similarities and differences between the Gulf Stream and Kuroshio Extension systems.

One finding of note was the strong evidence based on several groups' results that the WBC sea surface temperature (SST) fronts project onto the atmospheric boundary layer, affecting surface winds and cloud formation. Several groups furthermore showed evidence that affects of the sea surface temperature (SST) fronts appear to extend beyond the atmospheric boundary layer, to the top of the troposphere. In particular, analyses were presented showing that SST in the WBC regions influences the location of the storm tracks at low-levels. Much of the observed impact of the WBCs on the atmosphere has been derived from analyses of QuikSCAT sea-level winds, which provide the best coverage of surface winds at sufficiently small scales of any existing satellite measurement system. This led to discussions about the difficulties in observing the deep response of the troposphere to WBCs, especially during wintertime when extratropical storms are very energetic, and in observing the remote response, particularly to variations in the Gulf Stream. Modeling challenges were also discussed, as were recommendations for how WBC regions should be monitored for improved climate predictions.

Several action items resulted from the workshop and WBC WG. A web page (http://www.cdc.noaa.gov/WBC/) has been created that displays atmosphere and ocean fields relevant for the study of the Gulf Stream and Kuroshio Extension. A special issue of the Journal of Climate is planned that will include more than 20 studies presented at the workshop and two review papers on frontal-scale and large-scale air-sea interaction in WBC regions. The working group is drafting a Community White Paper (CWP) for the OceanObs09 conference titled "Monitoring ocean – atmosphere interactions in western boundary current extensions". The first draft of this CWP will be posted at http://www.oceanobs09.net for public comment after March 31, 2009. Finally, a set of metrics for evaluating climate models is being developed.

northwest of its counterpart in the control simulation. More striking, and presumably more significant from a dynamic perspective, is the prominence of the warm front for the storm in the cold SST run. We follow up on this point later.

The differences in the low-level thermodynamic structure between the simulated storms, as illustrated by the 925 hPa air temperatures presented above, can be related to the effects of the SST on the surface heat fluxes. As would be expected, the greater the SST, the greater the surface heat fluxes (not shown), and hence the warmer and more moist the ABL. It is less obvious that variations in SST should be manifested so prominently in the relatively cold air to the north and west of the simulated storm centers. This result is consistent, however, with the idea that the surface fluxes in situations of positive surface layer buoyancy (i.e., warm ocean/cool air) will tend to be greater than those in situations of negative buoyancy, given equal SLP gradients and magnitudes of air-sea thermodynamic differences, because of the greater low-level turbulence and higher transfer coefficients in the former case. In other words, the warm, southerly flow is more insulated from the effects of the cool ocean below than is the cool flow over a relatively warm surface. The simulations for the present case are consistent with this idea; note that air of 14° C at 925 hPa extends just past 45° N in the warm sectors of all three simulated storms, while the cool (6-8° C) air west of the storm extends less (more) equatorward in the warm (cold) SST simulations.

It stands to reason that the deepest storm is associated with the simulation (the cold SST perturbation) that includes the strongest warm front. A stronger warm front generally implies greater low-level thermal forcing of upward motion and geopotential height falls to the northeast of the low center. This is where the thermal forcing is most effective for continued development of storms tracking to the northeast.

Summary and Discussion

A short series of high-resolution NWP model experiments have been used to explore the atmosphere's sensitivity to SST during and immediately after a case of tropical to extratropical cyclone transition in the western North Pacific. These experiments consisted of a simulation with a control SST distribution, and a pair of simulations with imposed positive and negative SST perturbations centered off the east coast of Japan. Of the three simulations, the negative SST pertubation case yielded the strongest storm in the post-transition phase. This result, which may seem at least somewhat counter-intuitive, may be attributable to the cold SST case featuring a much more prominent warm front. The prominence of the warm front itself in this simulation is associated with reduced warming by the surface fluxes of the cold air wrapping around the north and west of the low center.

Some previous work on rapidly-developing mid-latitude cyclones (e.g., Kuo et al. 1991) has shown that the surface fluxes can be relatively unimportant to the rate of development during the rapidly deepening phase, and are instead more crucial for pre-conditioning the low-level air mass in the early stages of cyclogenesis. For the present case, this pre-conditioning was unnecessary in that the tropical origin of the cyclone implies pre-existing warm and moist low-level air in its vicinity during the early stage of its transition. As the storm moved north over cooler SST it became increasingly baroclinic, and at least for this particular case, the simulation with the cold SST perturbation yielded a solution that featured the greatest development after transition. We recognize that results based on a single case are tentative. With that in mind, we have used the observational record to compare various aspects of extratropical transitions during periods of warm versus cool SSTs. This material is outside the scope of the present article, but does support the results shown here, and will be included in a paper on this case we are preparing for Monthly Weather Review.

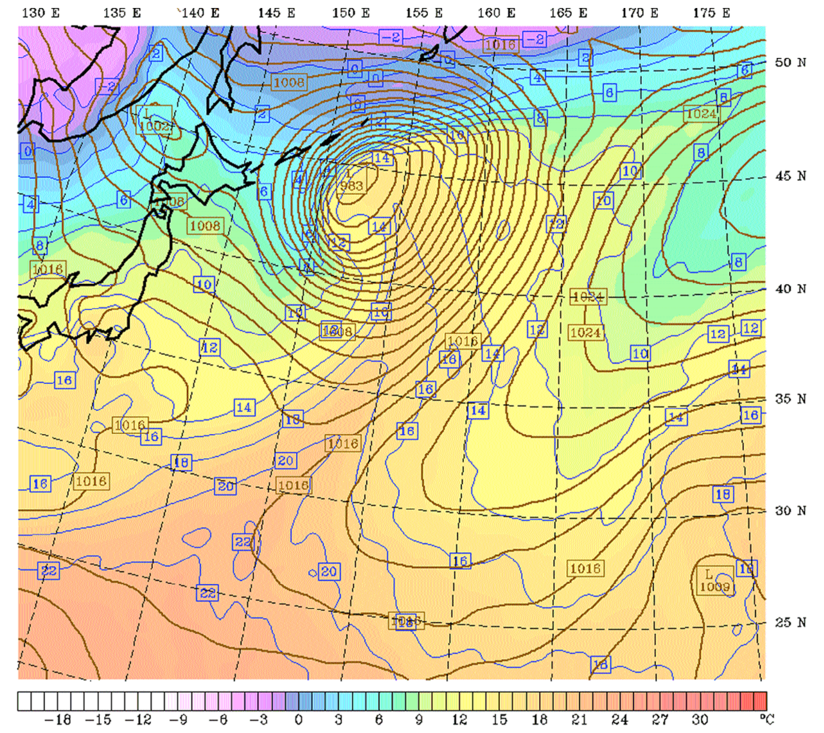

Figure 3 As in Fig. 1, but for the simulation with the cold SST perturbation.

The modification of storm track and structure by the regional SST has implications for the larger-scale atmospheric circulation. Our simulations reveal that the differences in storm structure were also manifested aloft. There are differences of ~40 m in the 500 hPa geopotential height between the perturbed and control simulations in the region of the storm; these signals propagated rapidly across the North Pacific (not shown). Forecasters have long posited that extratropical transitions in the western North Pacific are often followed by rather low predictability downstream over North America and beyond. Perhaps this lack of predictability results in part from errors and discrepancies in how the suite of operational NWP models handle air-sea interactions in the western North Pacific during transition events

References

Bond, N.A., and D.E. Harrison, 2000: The Pacific Decadal Oscillation, air-sea interaction and central north Pacific winter atmospheric regimes. Geophys. Res. Lett., 27, 731-734.

Chang, E.K.M., and I. Orlanski, 1993: On the dynamics of a storm track. J. Atmos. Sci., 50, 999-1015.

Kuo, Y.-H., R. J. Reed, and S. Low-Nam, 1991: Effects of surface energy fluxes during the early development and rapid intensification stages of seven explosive cyclones in the western Atlantic. Mon. Wea. Rev., 119, 457– 476.

Kushnir, Y., W. A. Robinson, I. Blade, N. M. J. Hall, S. Peng, and R. Sutton, 2002: Atmospheric GCM response to extratropical SST anomalies: Synthesis and evaluation. J. Climate, 15, 2233–2256.

Minobe, S., A. Kuwano-Yoshida, N. Komori, S.-P. Xie and R.J. Small, 2008: Influence of the Gulf Stream on the troposphere. Nature, 452, doi:10.1038/nature06690

Peng, S., W.A. Robinson, and M.P. Hoerling, 1997: The modeled response to midlatitude SST anomalies and its dependence on background circulation states. J. Clim., 10, 971-987.

Tokinaga, H., and Co-authors, 2006: Atmospheric sounding over the winter Kuroshio Extension: Effects of surface stability on atmospheric boundary layer structure. Geophys. Res. Lett., 33, L04703,doi:10.1029/2005GL025102.

Torn, R. D., and G. J. Hakim, 2009: Initial condition sensitivity of Western-Pacific extratropical transitions determined using ensemble-based sensitivity analysis. Mon. Wea. Rev., In Review

U.S. CLIVAR

Calendar of CLIVAR and CLIVAR-related meetings

Further details are available on the U.S. CLIVAR and International CLIVAR web sites: www.usclivar.org and www.clivar.org

WCRP Joint Scientific Committee Meeting
6-9 April 2009
College Park, Maryland
Attendance: Invited
http://www.clivar.org

European Geophysics Union General Assembly
19-24 April 2009
Vienna, Austria
Attendance: Open
http://www.egu.org

CLIVAR Working Group on Ocean Modeling: Panel Meeting
30 April - 1 May 2009
Exeter, UK
Attendance: Invited
http://www.clivar.org

CLIVAR Working Group on Ocean Modeling: Mesoscale Eddies Workshop
27-29 April 2009
Exeter, UK
Attendance: Open
http://www.metoffice.gov.uk/conference/mesoscale_workshop/

1st US Atlantic Meridional Overturning Circulation Meeting
4-6 May 2009
Annapolis, Maryland
Attendance: Open
http://www.AtlanticMOC.org/AMOC2009.php

World Ocean Conference
11- 15 May 2009
Manado, Indonesia
Attendance:Open
http://www.woc2009.org/home.php

NASA Ocean Vector Wind Science Team Meeting
18-20 May 2009
Woods Hole, MA
Attendance: Invited
http://coaps.fsu.edu/scatterometry/meeting/

CLIVAR Scientific Steering Committee Meeting
19-22 May 2009
Madrid, Spain
Attendance: Invited
http://www.clivar.org

CLIVAR/GOOS Indian Ocean Panel
3-5 June 2009
Le Reunion, France
Attendance: Invited
http://www.clivar.org

CLIVAR VAMOS (Varibility of the American Monsoon System) Meeting
3-6 June 2009
Puerto Rico
Attendance: Invited
http://www.clivar.org

NASA Earth System Science at 20
22-24 June 2009
Washington, DC
Attendance: Open

RAPID Open Science Meeting
7-10 July 2009
Edinburgh, Scotland
Attendance: Open
http://www.nerc.ac.uk/research/programmes/rapidwatch/events/090706/

VOCALS Science Meeting
12-14 July 2009
Seattle, Washington
Attendance: Invited

U.S. CLIVAR Summit
15-17 July 2009
Annapolis, Maryland
Attendance: Invited
Contact: http://www.usclivar.org

Joint IAMAS - IAPSO - IACS Meeting
19-24 July 2009
Montreal, Canada
Attendance: Open
http://www.iamas-iapso-iacs-2009-montreal.ca

GEWEX Conference
24-28 August 2009
Melbourne, Australia
Attendance: Open
http://www.gewex.org

U.S. CLIVAR
Climate Variability & Predictability
U.S. CLIVAR OFFICE
1717 Pennsylvania Avenue, NW
Suite 250
Washington, DC 20006

Subscription requests, and changes of address should be sent to the attention of the U.S. CLIVAR Office (cstephens@usclivar.org)

WCRP
World Climate Research Programme

U.S. CLIVAR contributes to the CLIVAR Program and is a member of the World Climate Research Programme

CLIVAR
Climate Variability & Predictability
World Climate Research Programme